Lab on a Chip

Cite this: DOI: 10.1039/c1lc20504h

www.rsc.org/loc

PAPER

Assessing the spatial resolution of cellular rigidity sensing using a micropatterned hydrogel–photoresist composite

Ian T. Hoffecker, Wei-hui Guo and Yu-li Wang*

Received 10th June 2011, Accepted 11th August 2011
DOI: 10.1039/c1lc20504h

The biophysical machinery that permits a cell to sense substrate rigidity is poorly understood. Rigidity sensing of adherent cells likely involves traction forces applied through focal adhesions and measurement of resulting deformation. However, it is unclear if this measurement takes place underneath single focal adhesions, over local clusters of focal adhesions, or across the length of the entire cell. To address this question, we developed a composite, chip-based material containing many arrays of 6.5 μm × 6.5 μm rigid adhesive islands, with an edge–edge distance of 8 μm, grafted onto the surface of a non-adhesive polyacrylamide hydrogel. This material is thus rigid within single islands while long-range rigidity is determined by the hydrogel. On soft gels, most NIH 3T3 cells spread only across two islands in a given dimension forming small stress fibers and focal adhesions. On stiff gels, cell spreading, stress fibers, and focal adhesions were indistinguishable from those on regular culture surfaces. We conclude that rigidity sensing is dictated by material compliance across the cell length and that responses to rigidity may be inhibited at any point when large substrate strain is encountered during spreading. Our finding may serve as a guideline for the design of biomaterials for tissue engineering.

Introduction

The rigidity of cell substrates dictates the deformation in response to traction forces applied by adhered cells and has a profound impact on cellular processes like migration, spreading, structural organization, growth, and differentiation.[1] Such influence has become an important consideration in both understanding pathological conditions particularly cancer metastasis,[2,3] and in the design of scaffold materials for supporting regenerative therapies such as wound healing and tissue engineering.[4]

Rigidity is measured by detecting material strain in response to applied mechanical forces.[5] For adherent cells like fibroblasts, the sensing involves focal adhesions, which transmit cytoskeletal contractile forces to the substrates and likely detect the strain through associated signal transduction enzymes and mechano-sensitive components.[1,6] However, an important question is whether rigidity detection is confined locally to areas near individual focal adhesions, or is dependent on the strain across the length of the cell as implicated by wrinkling films.[7]

Previous observations may be interpreted as supporting either a short- or long-range mechanism of rigidity sensing. The protein composition of focal adhesions, including components for both force transmission and sensing, appears self-sufficient for localized rigidity sensing as is supported by studies employing sub-micron beads. The effective rigidity of microscopic adherent beads, controlled by applying mechanical forces using either optical traps or magnets to counter traction forces exerted on the beads, was sufficient to affect local assembly of focal adhesions and actin filament bundles.[8,9] In addition, the turnover and density of integrins inside single focal adhesions appeared sufficient for sensing the spacing of adhesive ligands and substrate rigidity.[10]

Other studies have suggested the existence of contraction dipoles or lateral forces around single focal adhesions, which may be used for sensing rigidity in a local region of several focal adhesions.[11,12] However, the opposite conclusion may be reached from experiments with adherent cells placed on flexible pillars composed of relatively rigid polydimethylsiloxane (PDMS[13,14]), where cells responded not to the inherent rigidity of the materials but to the bending flexibility of the pillars, analogous to responses to homogeneous soft materials.[15] This suggests that the domain for rigidity sensing must be larger than the area of the pillars (1–2 μm in diameter).

Herein, we report a novel technique for micropatterning substrate rigidity, with the goal of distinguishing cellular sensitivity to micro-scale rigidity from cell-scale rigidity. This method was used to generate an elastic hydrogel base with arrays of stiff islands grafted onto the surface. While a previous study has micropatterned islands of the photoresist on elastic materials for the purpose of measuring traction forces,[16] the elastic material

Department of Biomedical Engineering, Carnegie Mellon University, Pittsburgh, PA, 15219, USA. E-mail: yuliwang@andrew.cmu.edu

used (polydimethylsilane) was too stiff for the present purpose. Using our method, the islands may move either easily (with a $G' < 500$ Pa) or hardly (with a $G' > 10\,000$ Pa) relative to each other upon the application of shear forces, while the islands themselves remain intrinsically rigid. This material allowed us to determine whether adhesive fibroblasts reacted to the intrinsic rigidity of the islands or to the bulk rigidity of the base hydrogel with cellular focal adhesions restricted to the rigid islands only.

Results and discussion

Reversible dehydration and rehydration of polyacrylamide hydrogels were exploited to allow for islands of the SU-8 photoresist to be cast over the surface in its dehydrated state. Patterns can be produced by tailoring the photomask used in selective exposure of the SU-8 photoresist (Scheme 1). The resolution allowed the generation of 4 × 4 arrays of 6.5 μm × 6.5 μm square islands separated by an edge-to-edge distance of 8 μm to cover an area of 50 μm × 50 μm, which is close to the average spread area of NIH 3T3 cells on unpatterned surfaces of the SU-8 photoresist.[17] This design was chosen in order to allow spreading fibroblasts to reach out and straddle multiple islands[18] while individually large enough to permit formation of multiple focal adhesions per island. By varying the concentration of acrylamide and bis-acrylamide, the rigidity of the base layer hydrogel may be controlled over a wide range. Control substrates of solid 50 μm × 50 μm SU-8 islands were also fabricated according to the same procedure.

This composite material was designed to possess two size scales of rigidity. The rigidity of SU-8 itself is high with a shear modulus of approximately 1–2 GPa.[19] In contrast, the hydrogels underlying these rigid islands may be as soft as several hundred Pa, which allowed the islands to move easily upon the exertion of traction forces. The results obtained with a soft hydrogel ($G' \approx 290 \pm 14$ Pa; triplicate samples, 4 measurements per sample) were then compared with those with a stiff hydrogel ($G' \approx 10.4 \pm 1.8$ kPa; triplicate samples, 4 measurements per sample). Similar shear moduli were obtained before and after exposing the gels to the micropatterning procedure, indicating that the grafting of the photoresist and the associated dehydration–rehydration did not significantly change the mechanical properties of the hydrogel (see the Experimental section).

To test whether adherent cells respond either to the short-range rigidity within the stiff islands or to the long-range rigidity of the underlying hydrogel, NIH 3T3 cells were cultured overnight on the patterned substrates with either soft (~290 Pa) or rigid (~10.4 kPa) hydrogel bases with identically patterned arrays of SU-8 islands. Clear differences in spreading behavior were observed between the two conditions (Fig. 1A and B). Cells on substrates with soft bases typically spanned no more than a 2 × 2 portion of the available islands (average total number of islands occupied = 3.8 ± 0.2, $n = 50$; Fig. 1E and G), whereas substrates made from stiff hydrogel bases allowed many cells to spread over the entire 4 × 4 array (average total number of islands occupied = 10.6 ± 0.6, $n = 50$; $P < 10^{-11}$; Fig. 1E and G). Measurements of spreading area indicated an average of 417 ± 23 μm^2 ($n = 50$) on soft hydrogel bases (Fig. 1D and F), but 1680 ± 100 μm^2 ($n = 50$) on stiff bases (Fig. 1D and F; $P < 10^{-12}$). Control patterns of 50 μm × 50 μm solid SU-8 squares were covered entirely by cells (Fig. 1C). These responses were similar to those seen on uniformly soft or stiff materials.[20,21]

In addition to the spreading area, both focal adhesions and stress fibers are known to increase in size with increasing substrate rigidity.[1] As expected, focal adhesions were restricted to the adhesive islands (Fig. 2). Composite substrates with rigid hydrogel bases induced the formation of large focal adhesions (Fig. 2A and the inset), which showed the typical elongated morphology aligned with adjoining stress fibers. Focal adhesions were typically located along outer edges and particularly at the four corners of each array (Fig. 2A and the inset), but were generally absent on islands in the interior of the arrays. The distribution is consistent with that observed and reported on

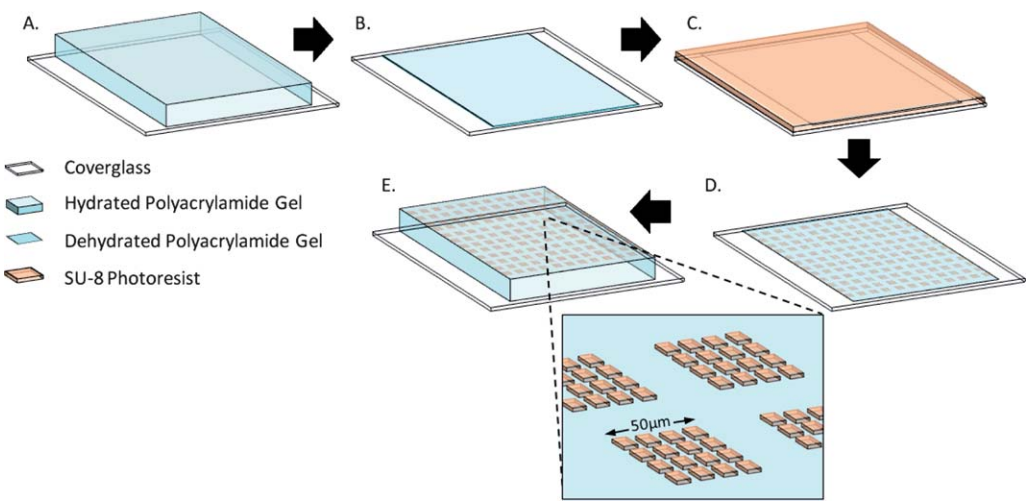

Scheme 1 Schematic representation of the island patterning procedure. A sheet of polyacrylamide hydrogels is first polymerized on top of a bind-silane activated coverglass (A). The hydrogel is air dried causing the hydrogel to collapse down against the coverglass (B). A thin layer of the SU-8 photoresist is then applied to the dried hydrogel *via* spin coating (C), followed by UV exposure through a photomask containing the pattern and development in the SU-8 developer to dissolve away unexposed regions of SU-8, leaving behind arrays of SU-8 islands (D). Immersion in PBS then allows the collapsed hydrogel to re-swell while maintaining the grafted SU-8 islands on the surface (E).

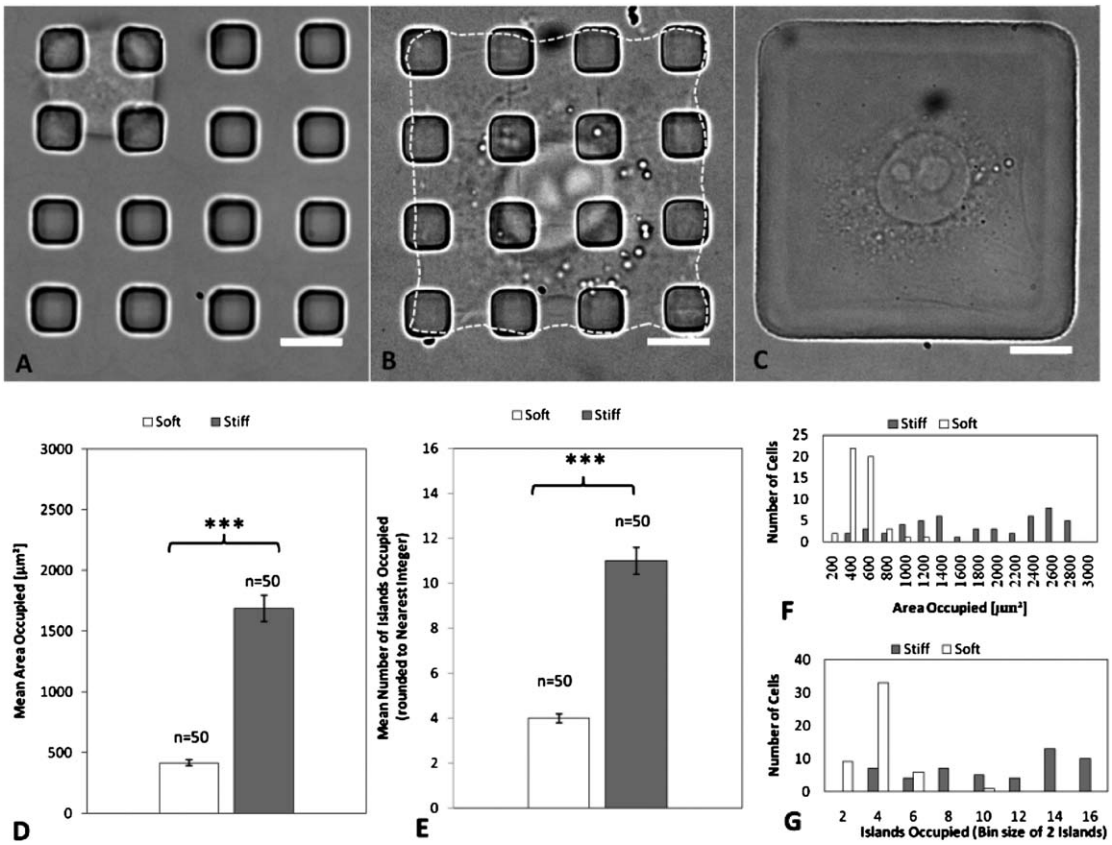

Fig. 1 Cell spreading on composite substrates. NIH 3T3 cells on composite substrates with a soft base and rigid islands assume a minimally spread morphology consistent with those on uniformly soft substrates (A). Cells on composite substrates with a rigid base and rigid islands show a highly spread morphology consistent with those on uniformly stiff substrates (B), as do cells on control substrates made from soft hydrogels patterned with 50 × 50 μm solid squares (C). Scale bars, 10 μm. Measurements of mean spread area (D), and mean number of islands covered (E) 18 hours after seeding show striking differences ($p < 10^{-12}$ and $< 10^{-11}$ respectively) between cells on islands with soft (3% acrylamide, 0.08% bisacrylamide: white bars) and stiff (12% acrylamide, 0.2% bisacrylamide: gray bars) hydrogel bases. Bars represent standard error of the mean. Histogram of the spreading area (F), and number of islands covered (G) 18 hours after seeding show that the great majority cells on islands with a soft base are able to cover only four islands, while those on islands with a stiff base are more variable in spreading area with a peak covering all the islands in the 2D array.

solid square islands (Fig. 2D).[22] The average area of focal adhesions on these substrates was 1.7 ± 0.1 μm² (Fig. 2E). Stress fibers in these cells were similarly well formed as a network throughout the cell.

In contrast, cells plated on composite substrates with soft hydrogel bases displayed only small focal contacts with no visible elongation, organization, or alignment (Fig. 2B). These focal contacts appeared randomly distributed as in cells during early stages of spreading. The average area occupied by each focal adhesion was much smaller than that on substrates with a stiff base (0.27 ± 0.01 μm²; $P < 10^{-28}$; Fig. 2E), and each island contained multiple focal contacts (insets of Fig. 2A and B). Similarly, only a few small, poorly organized stress fibers were found in these cells (Fig. 2E), analogous to those seen on homogeneous soft hydrogels.[1] Control cells on 50 μm × 50 μm solid squares or broad areas of SU-8 on soft hydrogels showed prominent focal adhesions and well-defined stress fibers (Fig. 2C and D). The contrasting results on stiff and soft hydrogel bases indicate that NIH 3T3 cells responded to the long-range rigidity even though the short-range rigidity was maintained at a constant high level.

Equally important is that the stiff islands were large enough to support the formation of multiple focal adhesions, indicating that short range rigidity between neighboring focal adhesions is insufficient to stimulate the formation of large focal adhesions as seen on uniformly stiff substrates. Alternatively, a large amount of slack anywhere along an axis of the cell may be sufficient to trigger dominant negative responses to prevent the formation of large stress fibers, focal adhesions, and spreading area, as suggested by the inability of cells to span more than two islands on soft bases.

The present results may be explained by a positive feedback mechanism that drives cell spreading and cytoskeletal organization. Newly plated cells show a limited spreading area, small scattered focal contacts, and fine, poorly organized actin filament bundles. The resistance of substrates to probing traction forces across the cell length was determined during spreading, such that strong resistance triggers strong positive feedback responses including the formation of progressively larger stress fibers, activation of actin flux at focal adhesions, and growth of focal adhesions that drive the increase in traction forces and spreading area.[23–25] This process continues until the cell reaches the limit of

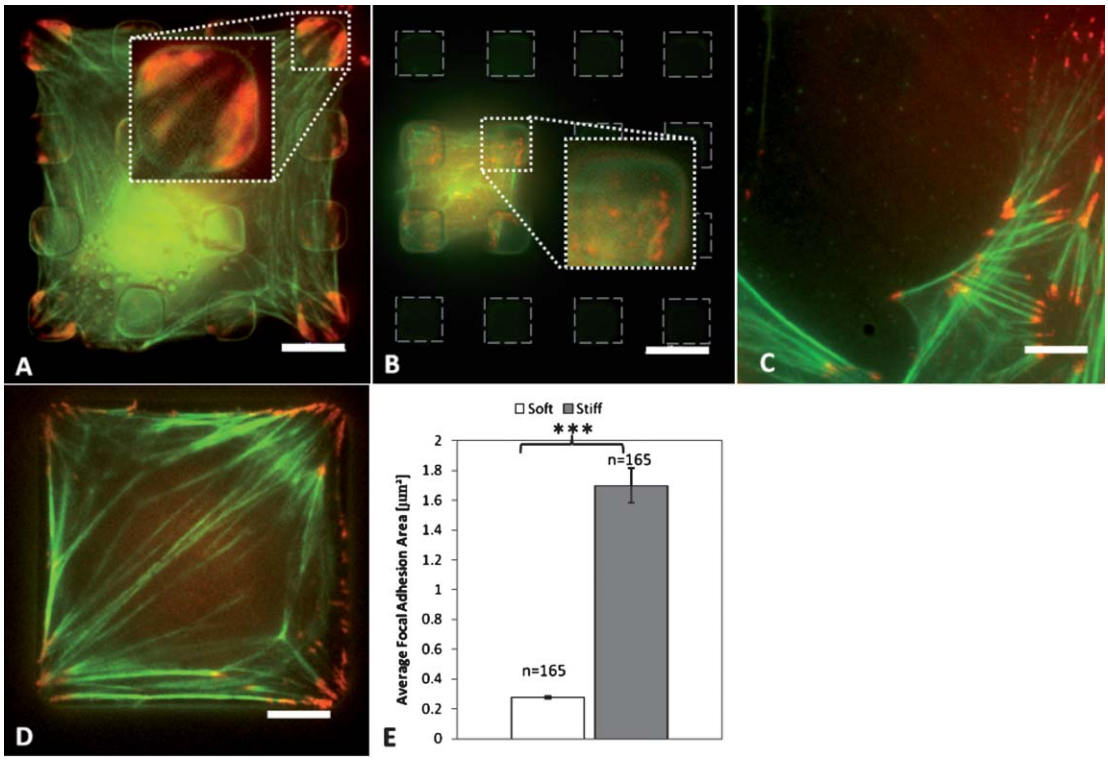

Fig. 2 Organization of F-actin (green) and paxillin (red) in cells on composite substrates. Cells on islands with a stiff hydrogel base exhibit clearly defined stress fibers and multiple, well elongated focal adhesions at the corners and aligned towards the cell center (A). The inset shows an enlarged view of focal adhesions. In contrast, cells on islands with a soft hydrogel base exhibit poorly defined stress fibers with multiple small, poorly organized focal contacts on each covered island (B). The inset shows an enlarged view of these small focal contacts. Control cells seeded on large strips of SU-8 spread freely over the surface and form well defined stress fibers and focal adhesions (C), as do cells seeded over 50 μm × 50 μm solid squares on soft gels (D). Bars, 10 μm. Measurements of average focal adhesion areas show a large, significant ($p < 10^{-28}$) difference between cells on substrates with a soft base (0.28 ± 0.01 μm^2) and those on a stiff base (1.7 ± 0.1 μm^2; E). Error bars represent standard error of the mean, from 165 focal adhesions in five cells for each condition.

spreading. In contrast, the lack of such feedback on soft substrates would keep cells in a poorly organized and poorly spread state. The results with stiff islands on the soft base further suggest that large amounts of slack during the course of spreading is sufficient to inhibit the positive feedback and the progress of spreading reactions.

It is important to note that the present study probes the scale of rigidity sensing without addressing the minimal adhesion area required to trigger the responses to stiff substrates. As long as adhesion sites are well-anchored to resist traction forces and tension is maintained between the two ends of a spreading cell, the area of adhesion may be as small as what is required to support the formation of a focal adhesion. This is consistent with previous findings that cells are able to spread over a matrix of small islands.[26] In addition, it explains why localized forces applied through sub-micron sized beads were able to elicit responses similar to those caused by long-range rigidity. As long as the cell is strongly adhered to the substrate, external forces exerted through micron-sized adhesive beads would generate sufficient tension to stimulate local responses.

The present finding is significant both for understanding cellular behavior under physiological conditions and for designing materials for clinical treatments. For example, physiological environments are rarely chemically nor mechanically homogeneous. The present study suggests that the mechanical environment of a long-range soft scaffold may be maintained even if it is dotted with subcellular domains of rigid materials. Conversely, it implies that the mechanical stimulus of a long range rigid scaffold may be maintained despite the presence of subcellular domains of soft materials. In addition, the guidance of cell migration by substrate rigidity, known as durotaxis,[21] may be determined by gradients over the cellular scale and unaffected by subcellular-scale variability in rigidity.

Experimental

Hydrogel preparation

The general procedure for patterning hydrogels with arrays of photoresist islands is outlined schematically in Scheme 1. This procedure allows for patterning of 1–2 μm features on either soft or stiff hydrogels. First, a coverglass was activated with 3 μL mL^{-1} bind-silane (GE Healthcare, Waukesha, WI) in a solution of 95% ethanol and 5% glacial acetic acid to allow the grafting of polyacrylamide hydrogels during polymerization. Polyacrylamide hydrogels were then prepared as previously described.[27] Precursor solutions were made by mixing stock solutions of *N*,*N*′-methylenebisacrylamide (bisacrylamide) (2% bisacrylamide; Bio-Rad, Hercules, CA) and acrylamide monomers (40% acrylamide; Bio-Rad, Hercules, CA). The amount of

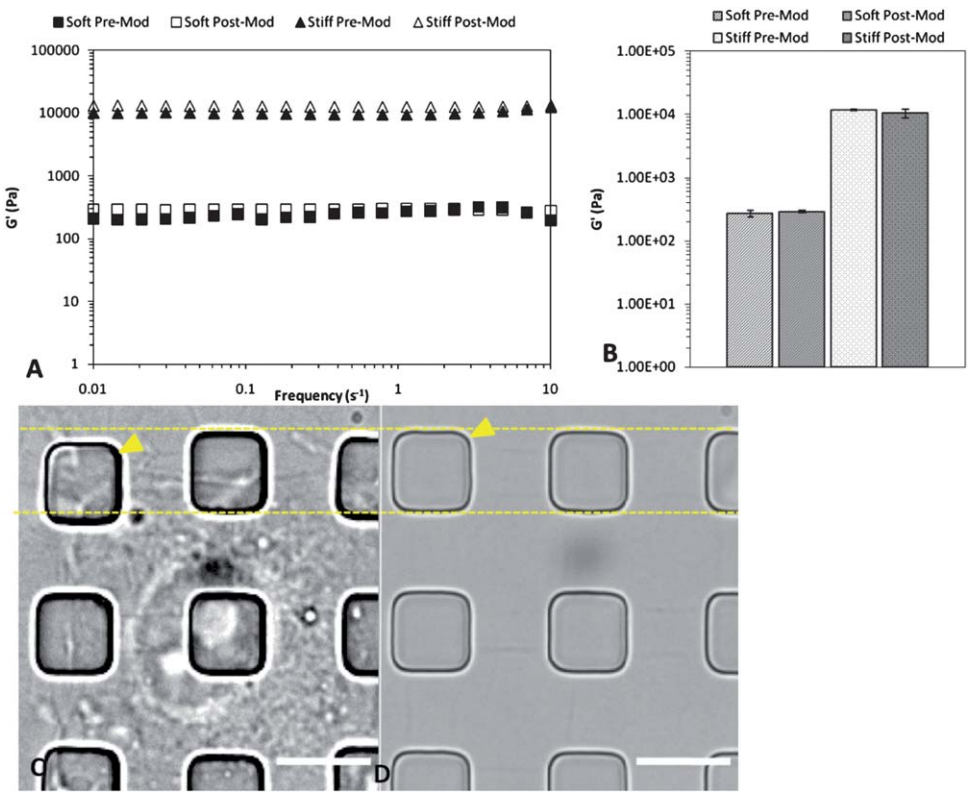

Fig. 3 Characterization of substrate elasticity. Mechanical properties of the polyacrylamide base layer are measured before and after over-layering with SU-8 using parallel plate rheometry (A). Graph shows representative measurements of the elastic shear modulus G' [Pa] at a constant strain of 0.01 as a function of shear frequency taken before and after hydrogel modification, for both soft (3% acrylamide, 0.08% bisacrylamide) and stiff (12% acrylamide, 0.2% bisacrylamide) hydrogels. Note the horizontal trends of G' as a function of frequency, which indicate the elastic quality of the samples. The average values of G' from multiple measurements of triplicate samples before and after the modification for micropatterning show no change in elasticity after drying and reswelling in the procedure for SU-8 overlay (B). Error bars represent the standard error of the mean. To verify the elastic recovery of hydrogels with SU-8 islands on the surface, cells are allowed to adhere to the islands and exert traction forces overnight (C). Strain of the hydrogel is evident (C, lines and arrows). Upon removal of the cells with trypsin, the displaced islands return to their initial positions to restore the regularity of the pattern, illustrating elastic properties of the gel and no slippage between island and hydrogel (D, lines and arrows). Scale bars, 10 μm.

acrylamide and the ratio of bisacrylamide to acrylamide control the rigidity of the hydrogel—a mixture of 3% acrylamide and 0.08% bisacrylamide was used for soft gels and a mixture of 12% acrylamide and 0.2% bisacrylamide was used for stiff gels. These solutions were degassed for 30 minutes before the initiation of polymerization with ammonium sulfate and *N*,*N*,*N*′,*N*′-tetramethylenediamine (TEMED) at concentrations of 0.06% (w/v) and 0.04% (v/v), respectively. A 20 μL drop was pipetted onto the activated coverglass and then covered with a 25 × 25 mm square coverglass (No. 1, 25 mm × 25 mm; Corning Life Sciences) pretreated with hydrophobic RAIN-X (SOPUS Products, Houston, TX) to facilitate subsequent removal. The reaction was allowed to proceed for 1 hour at 25 °C, and the resulting hydrogels were air dried vertically for 1 hour after removing the top coverslip (Scheme 1A and B).

Micropatterning

Arrays of rigid islands were created on dried hydrogels using the epoxy-based negative photoresist SU-8 2000 (Microchem, Newton, MA). Micropatterning was conducted according to the protocol of the manufacturer to produce features <3 μm in height. Coverslips with dried hydrogel were baked at 95 °C for 1 min before and after coating with 300 μL of SU-8 with a spin coater at 5000 rpm for 20 seconds (WS-6505-6NPP-LITE, Laurell Technologies, North Wales, PA; Scheme 1C). The coverslips were then exposed to ultraviolet light (360 nm, 100 mJ cm^{-2}) underneath a photomask with designed patterns (HTA Photomask, San Jose, CA), then baked for another 1 minute at 95 °C before immersion in the SU-8 developer (Microchem, Newton, MA, USA) for 90 seconds to yield the pattern (Scheme 1D). Developed coverslips were rinsed twice with 95% ethanol (Pharmaco-AAPER, Sherlbyville, KY, USA), and baked at 95 °C for 4 hours to ensure removal of any residual developer and mitigation of potential risk of cytotoxicity. Finally, the hydrogel was allowed to rehydrate in phosphate buffered saline (PBS; Scheme 1E) for 1 hour. Binding between the hydrogel and islands was stable enough such that the composite substrates lasted for at least three weeks upon storage.

Cell culture

NIH 3T3 mouse fibroblasts (ATCC, Rockville, MA, USA) were incubated at 37 °C in Dulbecco's Modified Eagle Medium (DMEM; Invitrogen) containing 10% donor adult bovine serum (Thermo-scientific), 2 mM L-glutamine, 50 μg mL^{-1}

streptomycin, and 50 μg mL^{-1} penicillin (Gibco BRL, Gaithersburg, MA, USA), under humidified atmosphere composed of 95% air and 5% carbon dioxide. Prior to plating cells, substrates were sterilized for 20 minutes under the germicidal lamp of a tissue culture cabinet. PBS was removed and replaced with cell culture media and allowed to equilibrate with the hydrogel. These media were then replaced with fresh media and incubated for 1 hour prior to cell plating, in order to allow passive adsorption of serum proteins to the SU-8 islands.[28] Plated cells were allowed to spread for 18 hours before observation or fixation. While the SU-8 photoresist most likely allowed cell adhesion by adsorbing extracellular matrix proteins, improved control of cell adhesion may be achieved in future studies through surface activation with agents such as sulfo-SANPAH and conjugation with a defined matrix protein.[29] This would also allow adhesion to take place over the entire surface rather than confined to stiff islands.

Fixation and fluorescent labeling

Cells were rinsed with 37 °C PBS then fixed for 10 minutes. Fixation solution consisted of 4% formaldehyde (from 16% stock solution, Thermo-Scientific, Rockford, IL) in PBS with 0.1% Triton X-100 (Sigma-Aldrich). Immunofluorescence staining for paxillin was performed using 1 : 200 dilution of anti-paxillin polyclonal rabbit antibody (SC-5574, IgG, Santa Cruz Biotechnology, CA), and 1 : 200 fluorescent anti-rabbit antibody (Alexa Fluor 546, goat anti-rabbit, IgG (H + L) 2 mg mL^{-1}, Invitrogen) following the standard procedure. Actin stress fibers were counter-stained with fluorescein phalloidin (F-432, Molecular Probes, Eugene, OR).

Microscopy and image analysis

Images were taken using a Nikon Eclipse Ti inverted microscope (Nikon Instruments Inc., Melville, NY) with an Andor iXON EM charged coupled device camera (Andor Technologies, Belfast, North Ireland). Bright field images and fluorescence images were acquired using a Nikon 100×, 1.49 NA oil immersion objective lens. ImageJ software was used to measure the cell spreading area and focal adhesion area after manually tracing the areas of interest.

Rheological characterization

Rheological studies of the hydrogel were conducted using a Bohlin Gemini Advanced Rheometer (Malvern Instruments Inc., NJ). The gel was prepared on small circular coverslips following the same procedure as for cell culture, except that the gel was at a thickness of 500 μm. After zeroing the rheometer with a dummy coverslip, the hydrogel sample on a coverslip was loaded onto the rheometer and frequency sweeps at 25 °C were conducted in the hydrogel's elastic regime from 10 Hz to 0.1 Hz at a constant strain of 0.01 using parallel plate geometry. For each sample, 4 frequency sweeps were conducted to obtain an average shear modulus (Fig. 3A and B). To test the rheological properties of the hydrogel after micropatterning, the patterning procedure was applied to circular 500 μm thick gels but without UV exposure, which caused the entire layer of the SU-8 photoresist to be removed during development. The processed hydrogels were then allowed to swell before testing under the same conditions as for control samples.

To assess elastic recovery of the hydrogel upon prolonged exertion of traction forces, cells were cultured overnight on a composite substrate with a soft base (Fig. 3C). Island displacement was visible compared to arrays without cells. Upon removal of the cells with trypsin, all the islands returned to their original positions as indicated by the restoration of the distance between islands to that of arrays without cells, suggesting that the hydrogels maintained their elasticity and that there was no slippage of the islands on the hydrogel surface (Fig. 3D).

Conclusions

In summary, we developed a new photoresist-hydrogel composite material with micropatterned rigidity dependent on the location and size scale of measurements. NIH 3T3 cells seeded on this material with a soft base were able to span only a limited distance and number of islands despite the adhesive contact with intrinsically rigid photoresist islands. Likewise, focal adhesions and stress fibers were small and unorganized as opposed to those on stiff bases, or in cells on uniformly stiff substrates. Our observations suggest that cells sense rigidity across the entire length of the cell body rather than in small domains within or between single focal adhesions. This principle may allow composite materials with distinct domains of chemical and physical properties to be designed for optimal clinical treatments. Future studies using this material with different cell types such as epithelial and endothelial cells, myocytes, chondrocytes, or stem cells may reveal whether the present results represent a universal principle of mechanosensing for adhesive cells.

Acknowledgements

The authors wish to thank Amsul Khanal, Dr Susanna Steppan, and the Carnegie Mellon Colloids, Polymers, and Surfaces Laboratory for training and access to the rheometer, as well as Professor Lynn Walker for guidance on matters pertaining to rheology. This work was supported by a grant from the NIH GM-32476.

Notes and references

1 D. Discher, P. Janmey and Y. L. Wang, *Science*, 2005, **310**, 1139.
2 M. J. Paszek, N. Zahir, K. R. Johnson, J. N. Lakins, G. I. Rozenberg, A. Gefen, C. A. Reinhart-King, S. S. Margulies, M. Dembo, D. Boettinger, D. A. Hammer and V. M. Weaver, *Cancer Cell*, 2005, **8**, 241.
3 R. W. Tilghman, C. R. Cowan, J. D. Mih, Y. Koryakina, D. Gioeli, J. K. Slack-Davis, B. R. Blackman, D. J. Tschumperlin and K. T. Parsons, *PLoS One*, 2010, **5**, e12905.
4 S. J. Bryant, T. T. Chowdhury, D. A. Lee, D. L. Bader and K. S. Anseth, *Ann. Biomed. Eng.*, 2004, **32**, 407.
5 P. A. Janmey, P. C. Georges and S. Hvidt, *Methods Cell Biol.*, 2007, **83**, 3.
6 C. K. Miranti and J. S. Brugge, *Nat. Cell Biol.*, 2002, **4**, E83.
7 A. K. Harris, P. Wild and D. Stopak, *Science*, 1980, **208**, 177.
8 D. Choquet, D. P. Felsenfeld and M. P. Sheetz, *Cell*, 1997, **88**, 39.
9 N. Wang and D. E. Ingber, *Biophys. J.*, 1994, **66**, 2181.
10 B. Wehrle-Haller and B. Imhof, *Trends Cell Biol.*, 2002, **12**, 382.
11 U. S. Schwarz, N. Q. Balaban, D. Riveline, A. Bershadsky, B. Geiger and S. A. Safran, *Biophys. J.*, 2002, **83**, 1380.
12 J. P. Butler, I. M. Tolic-Norrelykke, B. Fabry and J. J. Fredberg, *Am. J. Physiol. Cell Physiol.*, 2002, **282**, C595.

13 J. L. Tan, J. Tien, D. M. Pirone, D. S. Gray, K. Bhadriraju and C. S. Chen, *Proc. Natl. Acad. Sci. U. S. A.*, 2003, **100**, 1484.
14 O. du Roure, A. Saez, A. Beguin, R. H. Austin, P. Chavrier, P. Siberzan and B. Ladoux, *Proc. Natl. Acad. Sci. U. S. A.*, 2005, **102**, 2390.
15 A. Saez, A. Buguin, P. Silberzan and B. Ladoux, *Biophys. J.*, 2005, **89**, L52.
16 N. Q. Balaban, U. S. Schwarz, D. Riveline, P. Goichberg, G. Tzur, I. Sabanay, D. Mahalu, S. Safran, A. Bershadsky, L. Addadi and B. Geiger, *Nat. Cell Biol.*, 2001, **3**, 466.
17 C. C. Mader, E. H. Hinchcliffe and Y. L. Wang, *Soft Matter*, 2007, **3**, 357.
18 D. Lehnert, B. Wehrle-Haller, C. David, U. Weiland, C. Ballestrem, B. A. Imhof and M. Bastmeyer, *J. Cell Sci.*, 2004, **117**, 41.
19 T. Fujita, K. Maenaka and Y. Takayama, *Sens. Actuators, A*, 2005, **121**, 16.
20 T. Yeung, P. C. Georges, L. A. Flanagan, B. Marg, M. Ortiz, M. Funaki, N. Zahir, W. Ming, V. Weaver and P. A. Janmey, *Cell Motil. Cytoskeleton*, 2005, **60**, 24.
21 C. M. Lo, H. B. Wang, M. Dembo and Y. L. Wang, *Biophys. J.*, 2000, **79**, 144.
22 K. K. Parker, A. L. Brock, C. Brangwynee, R. J. Mannix, N. Wang, E. Ostuni, N. A. Geisse, J. C. Adams, G. M. Whitesides and D. E. Ingber, *FASEB J.*, 2002, **16**, 1195.
23 C. A. Reinhart-King, M. Dembo and D. A. Hammer, *Biophys. J.*, 2005, **89**, 676.
24 A. D. Rape, W. H. Guo and Y. L. Wang, *Biomaterials*, 2011, **32**, 2043.
25 W. H. Guo and Y. L. Wang, *Mol. Biol. Cell*, 2007, **18**, 4519.
26 C. S. Chen, M. Mrksich, S. Huang, G. M. Whitesides and D. E. Ingber, *Science*, 1997, **276**, 1425.
27 K. A. Beningo, C. M. Lo and Y. L. Wang, *Methods Cell Biol.*, 2002, **69**, 325.
28 T. Sikanen, S. K. Wiedmer, L. Heikkilä, S. Franssila, R. Kostiainen and T. Kotiaho, *Electrophoresis*, 2010, **31**, 2566.
29 R. J. Pelham and Y. L. Wang, *Proc. Natl. Acad. Sci. U. S. A.*, 1997, **94**, 13661.